We are IntechOpen,
the world's leading publisher of
Open Access books
Built by scientists, for scientists

4,800
Open access books available

122,000
International authors and editors

135M
Downloads

Our authors are among the

154
Countries delivered to

TOP 1%
most cited scientists

12.2%
Contributors from top 500 universities

CLARIVATE ANALYTICS
BOOK CITATION INDEX
INDEXED

WEB OF SCIENCE™

Selection of our books indexed in the Book Citation Index
in Web of Science™ Core Collection (BKCI)

Interested in publishing with us?
Contact book.department@intechopen.com

Variance Analysis and Autocorrelation Function for 2D Fiber Lap Statistical Analysis

Jean-Yves Drean and Omar Harzallah

Additional information is available at the end of the chapter

Abstract

This chapter reports on the statistical analysis of 2D fiber lap using variance analysis and autocorrelation function. It begins with a short overview of the nonwoven processes showing the importance of lap and web formation. It then proceeds to describe the theory of the ideal fiber web. The real defects are taken into account based on random irregularity, periodic irregularity, and compound irregularity. To conclude, the chapter highlights the efficiency of this theoretical approach and its application on 2D fibrous material.

Keywords: Fiber lap, fiber web, textile processes, statistical analysis, variance analysis, autocorrelation

1. Introduction

Textile and nonwoven industries are fiber-based industries. They use both continuous fibers as filament yarns and/or short fibers as staple fibers. During the manufacturing processes, these fibers, very thin 1D elements, are transformed in oriented or random 2D laps or webs. Then, these products are converted in 1D end product as staple yarns or 2D end products as woven or knitted fabrics or nonwoven fabrics. The physical and mechanical properties of these end products strongly depend on the regularity of laps or webs. Therefore, an accurate knowledge of the web and lap formation as well as the associated theoretical approach are absolutely necessary.

2. Textile processes

The classical textile spinning process is based on Figure 1. First of all, staple fibers highly compacted in form of bales are opened with the help of a bale opening line. Moving through a coarse and a fine opener, the size of fiber tufts is reduced to be able to feed the carding machine chute. The chute delivers a lap of fibers to the carding machine feed rolls.
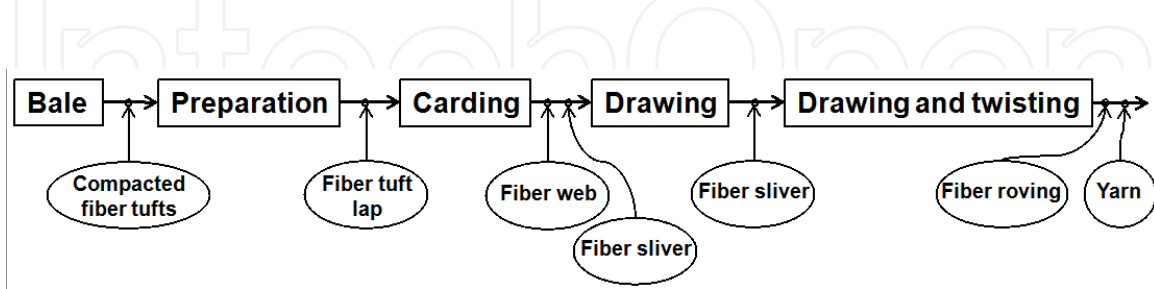

Figure 1. Scheme of classical textile process

In a second time, the carding machine, as shown in Figure 2, individualizes the fibers tufts and delivers the fibers in the form of a web. The web is then condensed in a form of sliver.
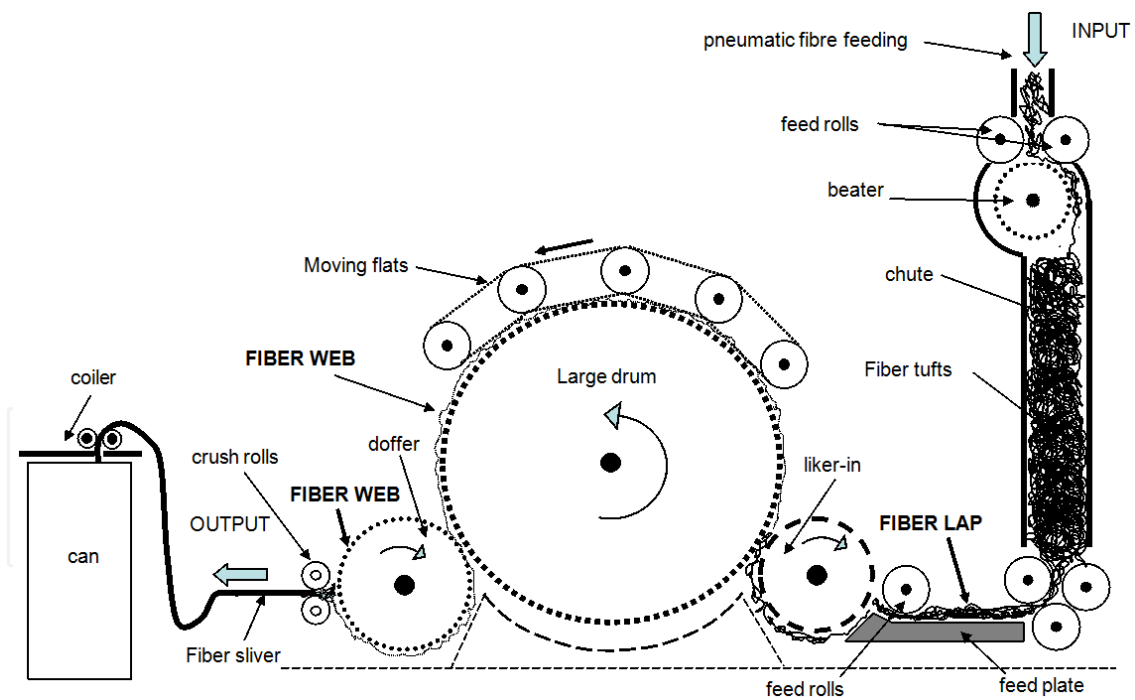

Figure 2. Carding machine

The sliver goes through a drawing frame and a roving frame which produces slivers which are drawn and twisted on a spinning machine, that is, ring spinning frame. The quality of the final product strongly depends on the efficiency of the carding operation. It can be noticed that this efficiency is strongly correlated to the quality and the evenness of both the fed lap and
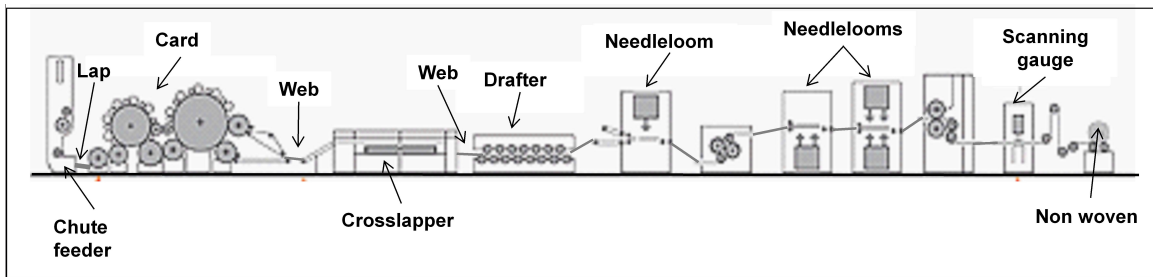
Figure 3. Drylaid needle-punched nonwoven line (Doc. ANDRITZ)

delivered web. An exact knowledge of the quality of these 2D textiles is absolutely necessary [1,16,17].

3. Nonwoven processes

Nonwoven materials can be considered as "**sheet or web** structures bonded together by entangling fibers or filaments, by various mechanical, thermal and/or chemical processes. These are made directly from separate fibers or from molten plastic or plastic film [1]" or as "a manufactured sheet, **web or mat** of directionally or randomly orientated fibers, bonded by friction, and/or cohesion and/or adhesion, excluding paper and products which are woven, knitted, tufted, stitch-bonded incorporating binding yarns of filaments, or felted by wet-milling, whether or not additionally needled [2]". As above defined, the web formation is a very important part of the nonwoven processes.

Nonwoven production systems are normally based on deposition or laying the fiber material or extruded thermoplastic polymers on a forming or conveying surface. The physical environment at this phase can be dry, quenched in air, wet, or molten – drylaid, wetlaid, or spun [3].

3.1. Nonwoven formation

In a general point of view, there are three main methods for nonwoven forming:

• The drylaid system with carding or airlaying

• The wetlaid system

• The polymer-based system, which includes spunlaying (spunbonding) or specialized technologies like meltblown, or flashspun fabrics [4]

The following chapter presents a non-exhaustive overview of a nonwoven manufacturing process.

3.2. Drylaid nonwoven

The drylaid nonwoven process consists in fiber preparation, web formation, web bonding, and stabilization (Figure 4).

The fiber preparation is close to classical textile industry staple fiber preparation including bale opening, blending, coarse, and fine opening. Then the web forming machine is fed with the help of a chute in case of short staple fibers or with the help of a hopper in case of long staple fibers. The fibers fed by a chute or hopper condensed into the form of a lap are introduced into a carding machine. The carding machine separates fibers, starts the process of individualization, and delivers the fibers in the form of a web [24,25].

The web is then formed into the desired web structure by layering the webs extracted from the carding machine. Based on the final chosen weight and web structure, the layering can be completed by using longitudinal layering, cross layering, or perpendicular layering.

Web strengthening can be done mechanically with the help of needle punching which consists in bonding nonwoven web by mechanically interlocking the fibers through the web using barbed needles (Figure 4), with the help of stitch bonding which consists in consolidating fiber webs using knitting elements or with the help of hydro-entanglement which consists in locking the fibers together using fine high pressure water jets directed across the web.
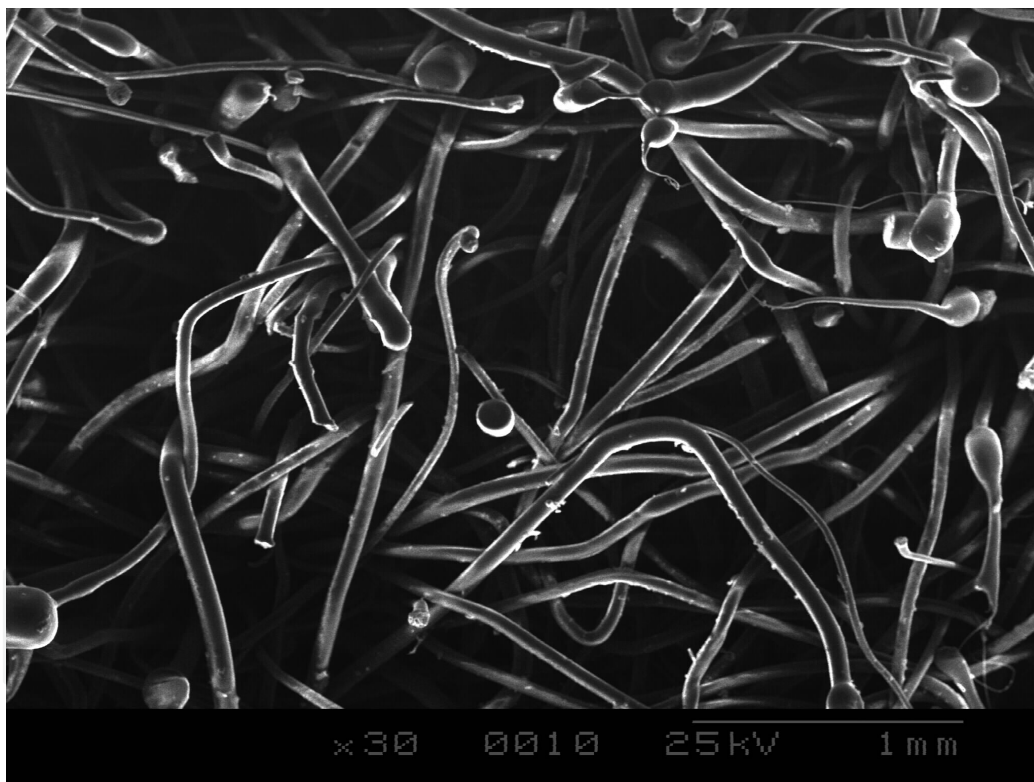
Figure 4. SEM photomicrograph of needle-punched nonwoven (natural and synthetic fibers)

Mechanical bonding can be replaced with web chemical bonding which consists in applying the chemical binder to the web and curing it.

In case of thermoplastic and thermostable fiber blend web, the strengthening can be achieved by thermal bonding.

3.3. Wetlaid nonwovens

This method relates to paper-based nonwoven fabrics which are manufactured by suspending short length fibers in water and pumping the suspension over a moving mesh in order to form a fibrous **web** [3].

Figure 5 is a schematic illustration of wetlaid technique. The blades of a very strong mixer transform fibers, wood pulp, and water to a perfect slurry suspension. Webformer deposes the suspension over the screen, and depending on the application of nonwoven, it will pass through a suitable bonding stage. Finally, nonwoven will be dried and wound up.
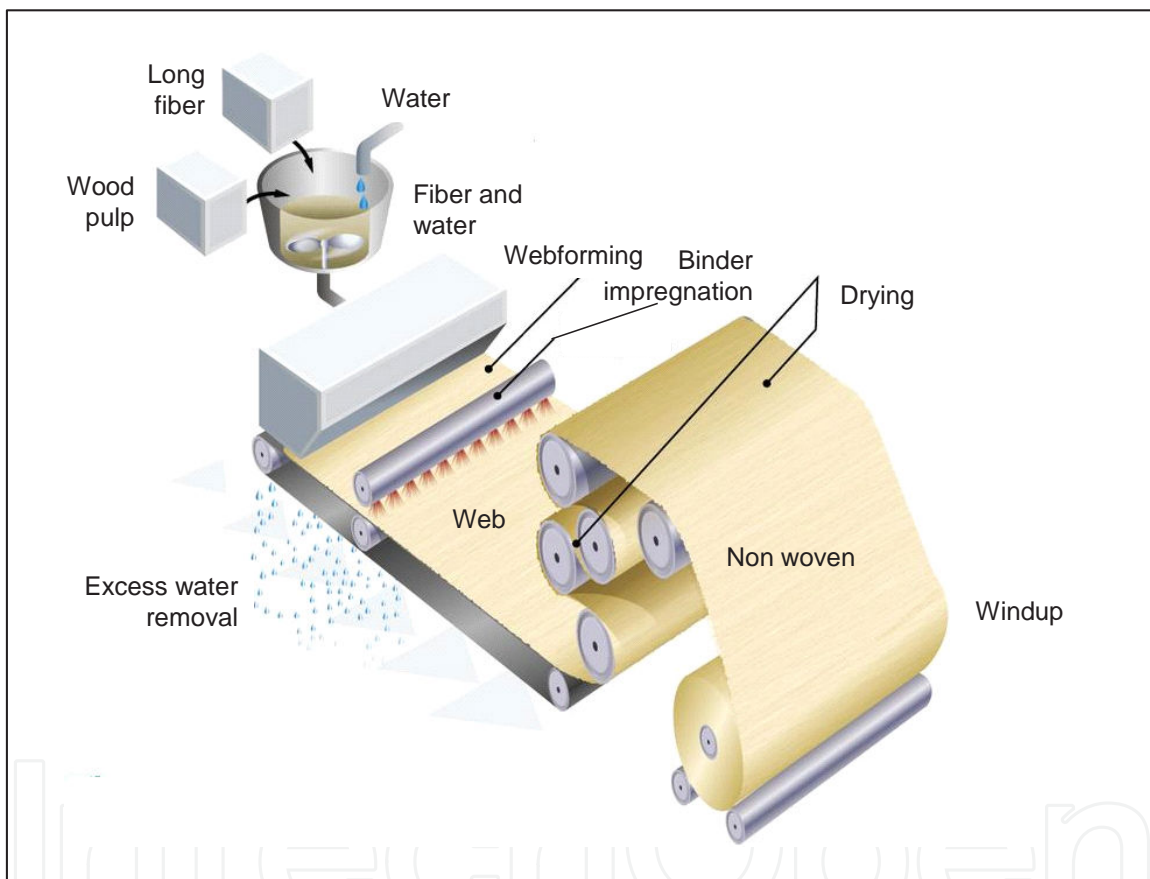

**Figure 5.** Wetlaid web formation [www.edana.org]

All fibers which are dispersible in fluids and do not dissolve can be transformed into a **web** form by using the wetlaid method. One of the main advantages of the wetlaid method is a very good product homogeneity due to the very good homogeneity of the **web**.

3.4. Meltblown nonwoven

As mentioned before, the meltblown process belongs to the general category of polymer-laid nonwoven material. It has been defined as below:

"Meltblowing is a process in which, usually, a thermoplastic fiber forming polymer is extruded through a linear die containing several hundred small orifices. Convergent streams of hot air (exiting from the top and bottom sides of the die nosepiece) rapidly attenuate the extruded polymer streams to form extremely fine diameter fibers (1–5 mm). The attenuated fibers are subsequently blown by high-velocity air onto a collector conveyor, forming a fine fibered self-bonded nonwoven meltblown **web** [1,4]." Figure 6 shows the schematic illustration of meltblown process.
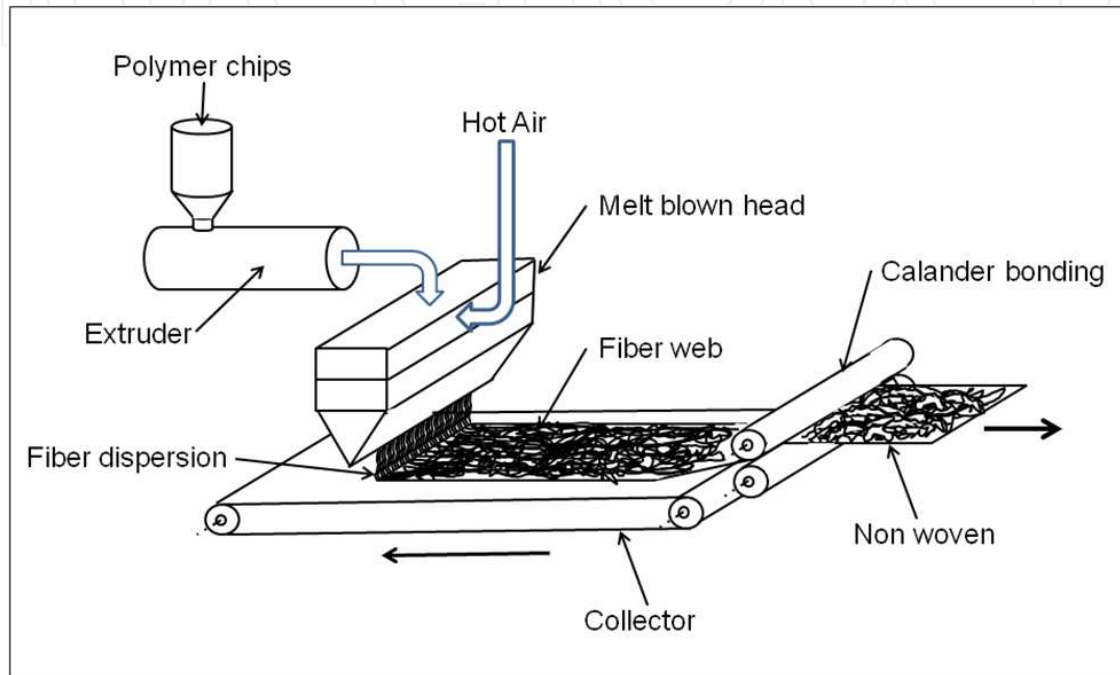

Figure 6. Meltblowing process; primary and secondary air flow and web formation

The main force that holds meltblown fibers together in a nonwoven structure is a combination of entanglement and cohesive sticking. Nonwoven produced by meltblown method have low to moderate strength. During the process, the fibers are drawn to their final diameters while still in the semi-molten state; there is no downstream method of drawing the fibers before they are deposited onto the collector, and this is the reason of moderate mechanical properties of meltblown nonwovens (Figure 7).

All the above-described processes are based on fibers and fibrous laps or webs. The characteristics of the web are determined by the mode of web formation which is related to web geometry. This web geometry takes into account fiber orientation (oriented or random), type of bonding, crimp, mass per unit area, and weight evenness and distribution.

The knowledge of the web geometry is very important because physical and mechanical properties are directly related to it. For instance, as far as geotextile properties are concerned, separation, reinforcement, stabilization, filtration, and drainage are related to the mass per unit area and the distribution of mass per unit area [5,23].
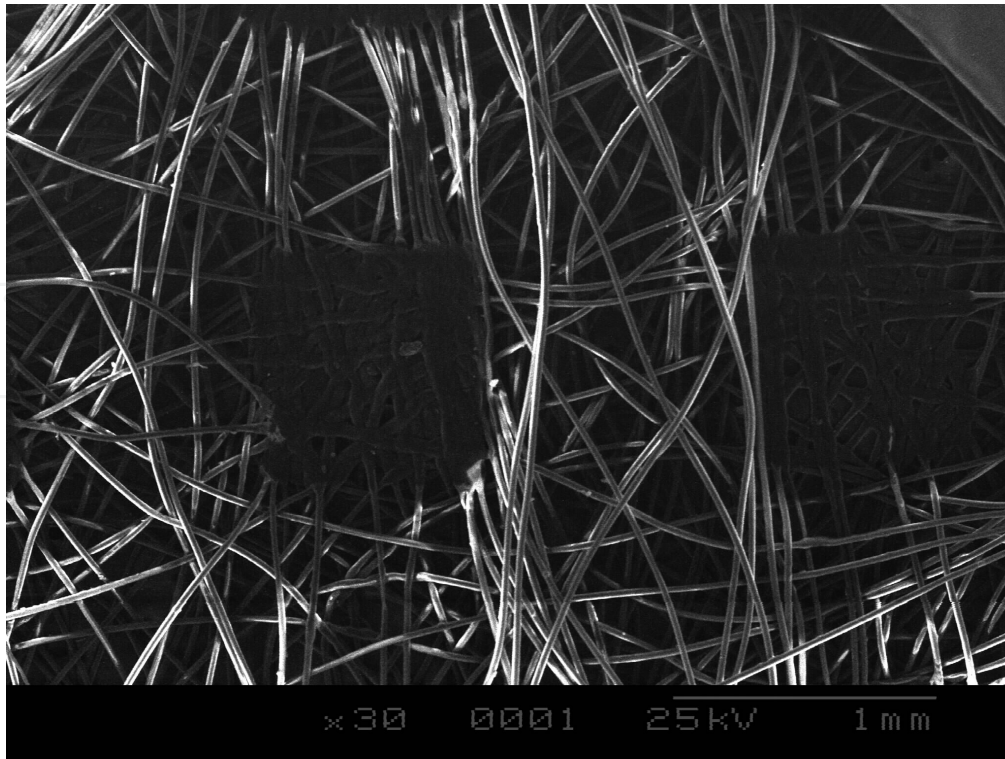
Figure 7. SEM photomicrograph of heat bonded meltblown nonwoven

The following paragraphs will present a theoretical approach of an ideal fiber web. This theoretical approach will simulate the real faults of the fiber-web forming-step during the industrial process, random irregularity, periodic irregularity, and compound irregularity.

4. Theoretical approach

4.1. The ideal fibrous web

In this chapter, the fiber web is split into several macro sample-elements; these elements have the same area A (Figure 8). The fiber web element area A is defined as the sum of fiber micro-strand da with $A = n \cdot da$, where n is the number of micro-elements in the macro-fiber-sample. The width L of the macro-web-element is considered constant. Its length is $l = \dfrac{A}{L}$ called cut length. Then, we suppose that $da = L \cdot dt$, where dt is the length of the fibrous micro-element located at the distance t from the strand origin. The abscissa origin 0 is located in the middle of the fiber web [6,7,8,9,26].

We assume that $\mu = \left(\dfrac{m}{da}\right)$ as the fiber strand area density of the fiber web (web manufactured by the textile machines); m is defined as the micro-elementary fiber-strand-mass. In this theory, the two random variables related to the cutting length l are μ and a, where μ can be described with the help of the usual statistical parameters as the mean and the variance [10,11].
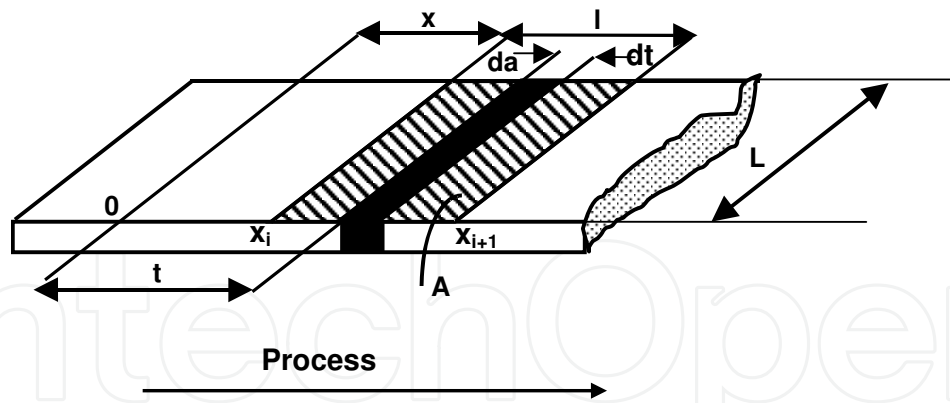
Figure 8. Scheme of an ideal fiber web

The unevenness of the area density of the fiber web can be characterized by the above-mentioned dispersion parameters which give an approach of the overall irregularity. The overall variance is denoted by the following limit conditions:

$$A \to \infty \quad and \quad da \to 0$$
$$n \to \infty$$

When the limits are taken, the variation coefficient of the fiber web and the overall variance can be written, respectively, as follows:

$$CV\left(0,\infty\right) = CV(\infty)$$
$$V\left(0,\infty\right) = V(\infty)$$

Taking into account that these values are not directly measurable, an estimation of the values can be calculated by extrapolation. Based on previous studies, [12,13,14,15,27], the mean and overall variance can be estimated as follows:

$$\bar{\mu}_i = \frac{\sum \mu_i}{n} = \frac{M}{A} \tag{1}$$

where M is the web-element-mass

and

$$\sigma_{\mu_i}^2 = \frac{\sum\left(\mu_i - \bar{\mu}_i\right)^2}{n} \tag{2}$$

4.2. $B(A)$ and $CB(A)$ functions

Let $B(A)$ be the variance between areas density of the ith macro-fibrous-element. Also, we define the macro-fiber-area density $\mu(x,\ A)$, where A is the mean value of the surface element and x is the abscissa (location of the element) [14,15,28,29].

$$\int_{y_0}^{y_0+L} \int_{x_0}^{x_0+A/L} \mu(x,y)dxdy = m(l,L) \tag{3}$$

We designate $E(\mu)$ as the average of the random variable $\mu(x,\ y)$; where E is the symbol of the mathematical expectation. $E(\mu)=E(\mu(x,\ y))$ can also be written as follows:

$$E\big(\mu(x,y)\big) = E\left[\int_{x_0}^{x_0+A/L} \int_{y_0}^{y_0+L} \mu(x,y)dxdy\right] \tag{4}$$

and based on the properties of the E operator:

$$E\big[m(l,L)\big] = \int_{x_0}^{x_0+A/L} \int_{y_0}^{y_0+l} E\big[\mu(x,y)\big]dxdy = l \cdot L \cdot E\big[\mu(x,y)\big] = A \cdot E\big[\mu(x,y)\big] \tag{5}$$

In the framework of this theory, the $B(A)$ variance between areas density is described by the second order moment as follows:

$$B\big[m(l,L)\big] = E\big[m(l,L) - E(\mu(l,L))\big]^2 \tag{6}$$

When Equation (5) is substituted into Equation (6), we obtain the following relationship:

$$B\big[m(l,L)\big] = E\left[\int_{x_0}^{x_0+A/L} \int_{y_0}^{y_0+L} \big(\mu(x,y) - E(\mu(x,y))\big)dxdy\right]^2 = E\left[\int_{x_0}^{x_0+A/L} \int_{y_0}^{y_0+L} \mu_c(x,y)dxdy\right]^2 \tag{7}$$

where $\mu_c(x,\ y)=\mu(x,\ y)-E(\mu(x,\ y))$

Then we set $u=\xi-x$ and $v=\eta-y$. The $B(A)$ function can be converted into a double integral assuming independence of position variables u and v. So, the $B(A)$ function can be written as follows:

$$B(A) = E\left[\int_{x_0}^{x_0+A/L} \int_{y_0}^{y_0+L} \int_{x_0}^{x_0+A/L} \int_{y_0}^{y_0+L} \mu_c(x,y)\mu_c(\xi,\eta)dxdyd\xi d\eta\right] \tag{8}$$

If we consider the two random functions $[\mu(x, y)-E(\mu(x, y))]$ and $[\mu(\xi, \eta)-E(\mu(\xi, \eta))]$, the Γ covariance function can be defined as follows:

$$\Gamma(u,v) = E\left[\left(\mu(x,y) - E\left(\mu(x,y)\right)\right)\cdot\left(\mu_c(x+u,y+v) - E\left(\mu_c(x+u,y+v)\right)\right)\right] \tag{9}$$

Hence $\Gamma(0, 0) = E[\mu(x, y) - E(\mu(x, y))]^2 = V[\mu(x, y)]$.

This allows showing that the covariance of the random variable $\mu(x, y)$ is a stationary random variable of second order [18,26]. In this case, the covariance is only depending on the difference of positions $(v + x)$ and on $(w + x)$:

$$(v+x)-(w+x) = v-w \tag{10}$$

Moreover, this covariance is an even function having the following property:

$$\Gamma(v-w) = \Gamma(w-v) \tag{11}$$

So, the new $B(A)$ equation can be defined as follows:

$$B\left[m(l,L)\right] = \int_{x=0}^{S/L}\int_{y=0}^{L}\int_0^{S/L}\int_0^{L}\Gamma(u,v)\,dv\,dw \tag{12}$$

The covariance is only a function of u where $u = v - w$; thus $B(A)$ can be reduced to a simple integral [27]. Thereby, the covariance function $B(A)$ can be rewritten in the following form:

$$B(A) = 2\cdot\frac{L^2}{A^2}\int_0^{A/L}\int_0^{L}\Gamma(u,v)\cdot\left(A/L - u\right)du\,dv \tag{13}$$

Let us now introduce the autocorrelation function [21]:

$$\rho(u,v) = \frac{\Gamma(u,v)}{\Gamma(0,0)} \tag{14}$$

Hence, a new form of the variance between areas density $B(A)$ can be expressed as follows:

$$B(A) = 2\Gamma(0)\cdot\frac{L^2}{A^2}\int_0^{A/L}\rho(u)\cdot\left(A/L - u\right)du \tag{15}$$

Then, let us use the initial function $B(A) = E[\mu(x, A) - E(\mu(x, A))]^2$ to estimate $B(0)$.

In the interval $[x_i, x_{i+1}]$ shown in Figure 1, if $A/L \to 0$, then $\mu(x, A) \to \mu(t)$. This means that the punctual area density is given by the following equation:

$$B(0) = E\left[\mu(t) - E(\mu(t))\right]^2 = V\left[\mu(t)\right] = \sigma^2_{\mu_i} \tag{16}$$

$\sigma^2_{\mu_i}$ representing the overall variance of the fiber-web-element.

Finally, $B(A)$ can be written as follows:

$$B(A) = 2 B(0) \cdot \frac{L^2}{S^2} \int_0^{S/L} \left(\frac{S}{L} - u\right) \rho(u) du \tag{17}$$

We designate $CB(A)$ as the variation coefficient associated to the between-area-density variance $B(A)$. Therefore:

$$CB^2(A) = \frac{B(A)}{E(\mu)^2} = \frac{2 \cdot CV^2_{\mu_i}}{A/L} \int_0^{A/L} \left(\frac{A}{L} - u\right) \rho(u) du \tag{18}$$

and $CV^2_\mu = \dfrac{\sigma^2_{\mu_i}}{E(\mu)^2}$ called the overall variation coefficient of the fiber web.

5. Discussion

5.1. Random irregularity

The fiber flocks length distribution is always considered of a great importance for textile laps and web processing. Nowadays, it is still a source of statistical interpretations more or less empirical, such as cumulative frequency diagram.

In the following part, the cumulative frequency function $q(\ell)$ of the fiber length ℓ is calculated by taking into account the shape of the most common distributions as isoprobable, equiprobable, and uniform distributions.

Based on textile sciences, these diagrams are usually represented by permuting the coordinated axes, that is, by plotting the value of the fiber length ℓ in the ordinate and $q(\ell)$ in abscissa, as shown in Table 1.

	Isoprobable distribution	Equiprobable distribution	Uniform distribution
Cumulative frequency diagram of the fiber length			
Mean length of fiber web flock	$\overline{\ell} = \ell_m = \ell$	$\overline{\ell} = \dfrac{\ell_m}{2}$	$\overline{\ell} = \dfrac{c+b}{2}$
Autocorrelation function: $\rho(u) = \dfrac{1}{\overline{\ell}} \cdot \int_u^{\ell_m} q(\ell)\,d\ell$			
$\dfrac{S}{L} = l \le \ell_m$	$\rho(u) = 1 - \dfrac{u}{\overline{\ell}}$	$\rho(u) = \left(1 - \dfrac{u}{2\overline{\ell}}\right)^2$	$\dfrac{A}{L} = l \le b$; $\rho_1(u) = 1 - \dfrac{u}{\overline{\ell}}$ $b < \dfrac{A}{L} = l \le c$; $\rho_2(u) = \dfrac{(c-u)^2}{c^2 - b^2}$
$\dfrac{A}{L} = l \ge \ell_m$	0	0	0

Table 1. Diagrams of distribution

The usual empirical criterion for the quality estimation of the fiber web is based on the shape of the diagram. If all fiber flocks have the same length $\ell = \ell_m = \overline{\ell}$ and same m mass, the diagram of cumulative frequency would obviously be a rectangle (Table 1); $\overline{\ell}$ and ℓ_m being, respectively, the mean and the maximum flock fiber length. This type of distribution is designated as "isoprobable". In case of a cumulative frequency of length distribution triangular shape, the distribution is considered an equiprobable distribution. Such a shape shows the presence of a linear unevenness of length. The combination the two previous distributions leads to define a new third distribution called "uniform". In this distribution, the fiber length decreases linearly between two values b and c as shown in Table 1. Considering the three above-described distributions, the calculated mean lengths are given in Table 1 and are, respectively, mathematically expressed as follows:

$$\overline{\ell} = \ell_m$$
$$\overline{\ell} = \frac{\ell_m}{2} \text{ and }$$
$$\overline{\ell} = \frac{c+b}{2}.$$

Based on the shape of the diagram of cumulative frequency, the function $q(\ell)$ can be defined. On the other hand, the autocorrelation function $\rho(\ell = u)$ of the fiber flocks is given by the following equation:

$$\rho(u) = \frac{1}{\bar{\ell}} \cdot \int_{\ell=u}^{\ell_m} q(\ell) d\ell \tag{19}$$

where ℓ_m is the length of the longest fiber flocks.

It can be highlighted that the autocorrelation function is a double integration of the histogram (frequency distribution function) of a fiber web numerical sample.

The cumulative frequency function $q(\ell)$ and the autocorrelation function exist only if the cut length of a fibrous web $l = \dfrac{A}{L}$ is small, that is, $l \leq \ell_m$ as clearly shown in Table 1. Otherwise if $\dfrac{A}{L} = l$ is large, $l \geq \ell_m$, we can demonstrate easily that $\rho(u) = 0$. Considering these parameters, the between-area-density variance $B(A)$ can be calculated using the following equation, if $l \leq \ell_m$:

$$B(A) = \frac{2B(0)}{l^2} \int_0^l (l-u) \cdot \rho(u) du \tag{20}$$

While, if $\dfrac{A}{L} = l$ is large, $l \geq \ell_m$, we have $\rho(u) = 0$. The function $B(A)$ takes the following expression:

$$B(A) = B(0) \left[1 - \frac{2}{l^2} \int_0^{\ell_m} (l-u) \cdot (1 - \rho(u)) du - \frac{2}{l^2} \int_{\ell_m}^l (l-u) du \right] \tag{21}$$

Then $B(A)$ and $CB^2(A)$ can be normalized:

$$\beta(A) = \frac{B(A)}{B(0)} = \frac{CB^2(A)}{CB^2(0)} \tag{22}$$

with $CB^2(A) = \dfrac{B(A)}{E(\mu)^2}$

For a fiber web having the **isoprobable distribution** of the fiber flocks, the normalized between-area-density variance $\beta(A)$ takes the following expressions:

$$\text{if } l \leq \ell_m \quad \beta(A) = \frac{B(A)}{B(0)} = \frac{CB^2(A)}{CB^2(0)} = \left[1 - \frac{l}{3\bar{\ell}} \right] \tag{23}$$

$$\text{if } l \geq \ell_m \ \ \beta(A) = \frac{B(A)}{B(0)} = \frac{CB^2(A)}{CB^2(0)} = \left[\frac{\overline{\ell}}{l} - \frac{\overline{\ell}^2}{3l^2} \right] \tag{24}$$

The difference between a "short" and a "long" fiber web element is shown by the diagrams of $\beta(A)$ in Figures 9 and 10. In case of $l \leq \ell_m$, the functions $B(A)$ and $CB^2(A)$ present straight segments in the interval $[0, \ell_m]$ as mentioned in Figures 9 and 10. The slope $\beta(A)$ curve at the origin is $-\frac{1}{3\overline{\ell}}$. It can be noticed that the two branches of the $\beta(A)$ graph are connected to point B coordinates $\left(\overline{\ell}, \frac{2}{3} \right)$.
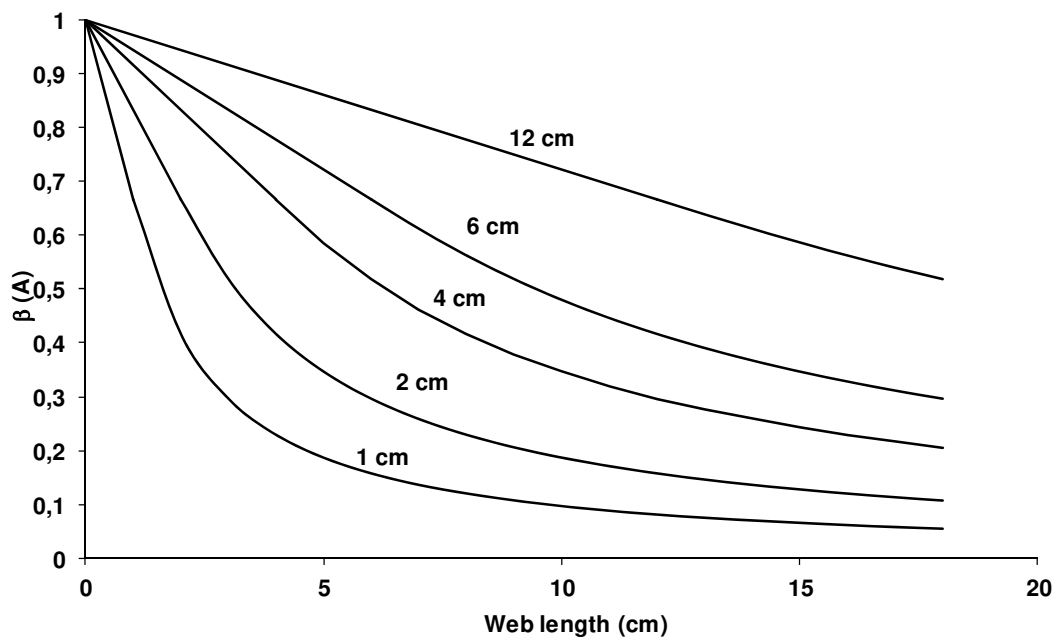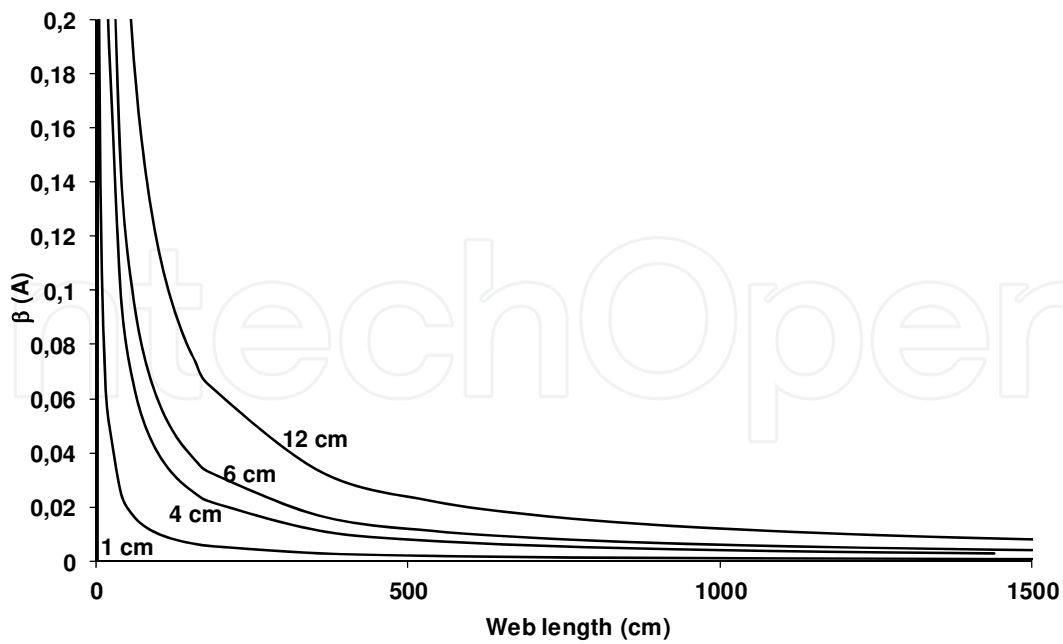

Figure 9. Short-term irregularity – between-area-density variance vs. fiber web length: Case of length isoprobable distribution

Otherwise, for the **equiprobable distribution**, the corresponding diagram has a triangular shape (see Table 1). By a similar calculation to the previous we obtain two expressions for $\beta(A)$:

$$\text{if } 0 \leq l \leq \ell_m \ \ \beta(A) = \frac{B(A)}{B(0)} = \frac{CB^2(A)}{CB^2(0)} = \left[1 - \frac{l}{3\overline{\ell}} + \frac{l^2}{24\overline{\ell}^2} \right] \tag{25}$$

$$\text{if } l > \ell_m \ \ \beta(A) = \frac{B(A)}{B(0)} = \frac{CB^2(A)}{CB^2(0)} = \left[\frac{4\overline{\ell}}{3l} - \frac{2\overline{\ell}^2}{3l^2} \right] \tag{26}$$

Figure 10. Long-term irregularity – between-area-density variance vs. fiber web length: Case of length isoprobable distribution

It can be noticed that the graph of $\beta(A)$ related to the equiprobable distribution is always above the one corresponding to the associated isoprobable distribution for the same ℓ (Figure. 11).

Finally, the $q(\ell)$ **uniform distribution** that has a trapezoidal shape (Table 1) has the mean and the variation coefficient respectively expressed [22] as follows:

$$\bar{\ell} = \frac{c+b}{2} \text{ and } CV\% = \frac{100}{\sqrt{3}} \cdot \left(\frac{c-b}{c+b}\right) \tag{27}$$

It can be noticed that if $b=c=\ell$ the distribution is isoprobable, then if $b=0$ and $c=2\ell$ the distribution is equiprobable.

In this case of uniform distribution, the cumulative frequency function and the autocorrelation function have, respectively, the following expressions:

$$\text{if } 0 \leq \frac{A}{L} = l \leq b, \ q_1(\ell) = 1 \text{ hence:}$$
$$\rho_1(u) = \frac{1}{\bar{\ell}} \int_l^{\ell_m=c} q(u) du = \frac{1}{\bar{\ell}} \int_l^b q_1(u) du + \frac{1}{\bar{\ell}} \int_b^c q_2(u) du \tag{28}$$

After integration $\rho_1(u)$ becomes:

$$\rho_1(u) = 1 - \frac{l}{\bar{\ell}} \tag{29}$$

$$\text{if } b < \frac{A}{L} = l \le c, \ q_2(u) = \left(\frac{c-l}{c-b}\right) \text{ hence:}$$
$$\rho_2(u) = \frac{1}{\overline{\ell}} \int_l^{\ell_m=c} q(u) du = \frac{(c-l)^2}{c^2-b^2}$$
(30)

$$\text{if } \frac{A}{L} > c, \ q_3(\ell) = 0, \text{ hence :}$$
$$\rho_3(u) = \frac{1}{\overline{\ell}} \int_a^\infty q(u) du = 0$$
(31)

According to the values of $\frac{A}{L}$, $\beta(A)$ takes the following expressions [28,29]:

$$\text{if } 0 \le \frac{A}{L} = l \le b \ \ \beta(A) = \left[1 - \frac{l}{3\overline{\ell}}\right]$$
(32)

$$\text{if } b < \frac{A}{L} = l \le c \ \ \beta(A) = \frac{2}{l^2} \cdot \left[\frac{lcb}{2\overline{\ell}} - \frac{b^2(3c-b)}{12\overline{\ell}} + \frac{(c-b)^3}{24\overline{\ell}}\left(\left(\frac{c-l}{c-b}\right)^4 - 4\left(\frac{c-l}{c-b}\right) + 3\right)\right]$$
(33)

$$\text{if } \frac{A}{L} > c \ \ \beta(A) = \frac{2}{l^2} \cdot \left[l\frac{(c^2+b^2+cb)}{6\overline{\ell}} - \frac{(c+b)(c^2+b^2)}{24\overline{\ell}}\right]$$
(34)

As shown in Figure 12, if $0 \le \frac{A}{L} = l \le b$, the functions $B(A)$ and $CB^2(A)$ present straight segments in the interval $[0, b]$. The slope of $\beta(A)$ curve at the origin is $-\frac{1}{3\overline{\ell}}$. Based on this figure, we can note that if $\frac{b}{c}$ is low while the flocks length variation coefficient is high, the slope of $\beta(A)$ decreases more slowly.

Considering the three above-described distributions, the random unevenness varies with the variation of the fibrous web length and as shown is Figures 9 and 10, if l increases, $\beta(A)$ decreases.

This can be explained by a greater possibility of compensating local irregularities in case of longer surfaces of fiber web. Normally, the $\beta(A)$ fiber web curve has a decreasing course, tending toward zero for $l \to \infty$.
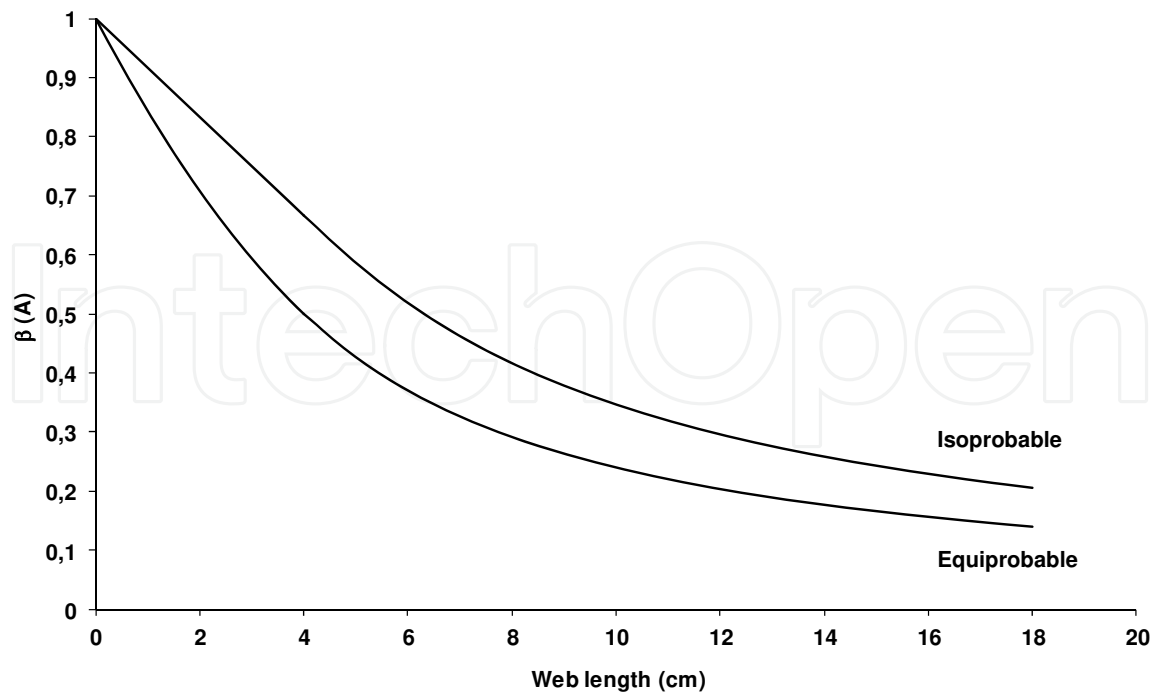
Figure 11. Comparison between the $\beta(A)$ curves of the isoprobable and equiprobable distributions for the same length ℓ
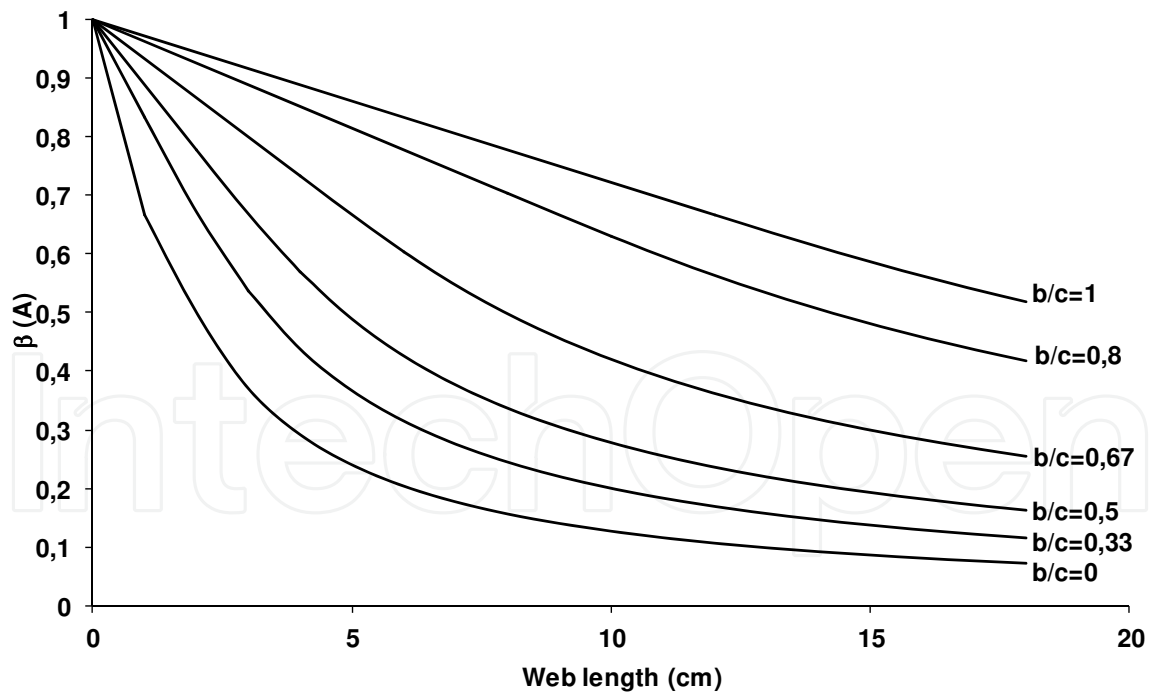

Figure 12. Short-term irregularity – between-area-density variance vs. fiber web length: Case of length uniform distribution

5.2. Periodic unevenness

We suppose that the area density of the fibrous web is defined as follows:

$$\mu(t) = \mu + a\cos(\omega t) \tag{35}$$

where μ: average area density, assumed constant

a: amplitude of the sinusoidal component irregularity

ω: pulsation of the sinusoidal component irregularity

We have seen that $B(A)$ can be written as follows:

$$B(A) = E\left[\frac{L}{A}\int_x^{x+A/L}(\mu(t) - E(\mu))dt\right]^2 \tag{36}$$

with $E(\mu(t)) = \mu$.

Hence by replacing $\mu(t)$ by its value:

$$B(A) = E\left[\frac{L}{A}\int_x^{x+A/L}a\cos(\omega t)dt\right]^2 \tag{37}$$

and finally after integration:

$$B(A) = \frac{a^2}{2}\cdot\frac{\sin^2\left(\dfrac{\omega\cdot A/L}{2}\right)}{\left(\dfrac{\omega\cdot A/L}{2}\right)^2} \text{ and } B(0) = \frac{a^2}{2} \tag{38}$$

$$B(A) = B(0)\cdot\frac{\sin^2\left(\dfrac{\omega\cdot A/L}{2}\right)}{\left(\dfrac{\omega\cdot A/L}{2}\right)^2} \text{ and the normalized for } \beta(A) = \frac{B(A)}{B(0)} = \frac{\sin^2\left(\dfrac{\omega\cdot A/L}{2}\right)}{\left(\dfrac{\omega\cdot A/L}{2}\right)^2}.$$

Hence we deduce the corresponding variation coefficient:

$$CB(A) = CB(0) \cdot \frac{\sin\left|\dfrac{\omega \cdot A/L}{2}\right|}{\left(\dfrac{\omega \cdot A/L}{2}\right)} \text{ and}$$

$$\gamma(A) = \frac{CB(A)}{CB(0)} = \frac{\sin\left|\dfrac{\omega \cdot A/L}{2}\right|}{\left(\dfrac{\omega \cdot A/L}{2}\right)} \ (\text{normalized form})$$

(39)

where $\omega = \dfrac{2\pi\,v}{\lambda}$ is the pulsation of the irregularity sinusoidal component

v represents the fiber flow velocity through the sensor

λ is the wavelength irregularity

The $\beta(A)$ and $\gamma(A)$ curves show a periodic-arches succession with a decreasing amplitude and a $\dfrac{\pi\lambda}{v}$ (Figures 13 and 14). The shape of these curves is totally different from those corresponding to the random distribution. This result is very significant for the production manager in order to detect the defects origin.
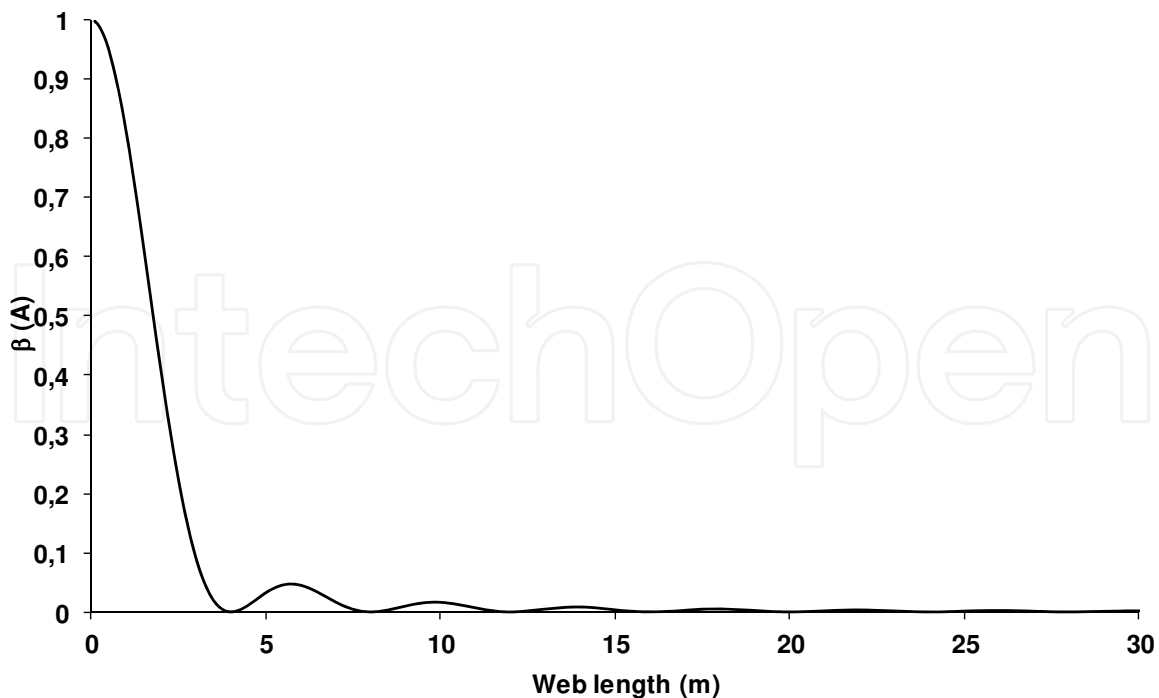

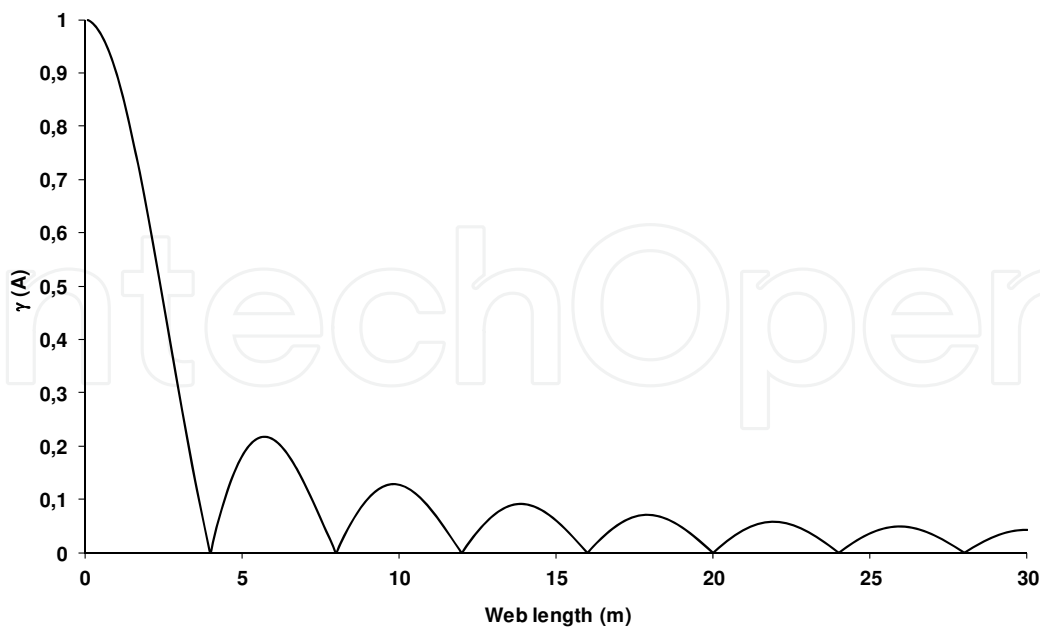**Figure 13.** Normalized between-area-density variance curve – periodic irregularity $\lambda = 4 \ m$

Figure 14. Normalized between-area-density variance coefficient curve – periodic irregularity $\lambda = 4 \ m$

5.3. Compound unevenness

In the above-mentioned development, we have intentionally unheeded the random compo-
nent and assumed the presence of only one type of periodic sinusoidal irregularity. In fact, the
random component is always present in the 2D textile fibrous structures and is existing; the
additional components are of several sinusoidal types generated by the manufacturing
process. That way, the periodic irregularity has to be split according to Fourier series [17] and
the composition of the $B(A)$ variance concerning the various components (random and
periodic) of the area density irregularity have to be calculated. The calculation is based on the
additivity property of variances of independent variables.

Firstly, only one type of sinusoidal periodic irregularity is taken in account as follows:

$$M(x) = \mu(x) + a\cos(\omega x) \tag{40}$$

where $\mu(x)$= random component of the area density of the fibrous web

$a\cos(\omega x)$= sinusoidal component of amplitude a and pulsation ω

Based on the law of additive covariances composition [26], we deduce the expression of the
autocorrelation function $\rho(u)$:

$$\rho(u) = \left(\frac{\sigma_a^2}{\sigma_\mu^2}\right) \cdot \rho_a(u) + \left(\frac{\sigma_p^2}{\sigma_\mu^2}\right) \cdot \rho_p(u) \tag{41}$$

Let $\eta = \left(\dfrac{\sigma_p^2}{\sigma_\mu^2} \right)$. With η being the weighting factor ($0 \leq \eta \leq 1$).

$$\rho(u) = (1-\eta) \cdot \rho_a(u) + (\eta) \cdot \rho_p(u) \tag{42}$$

with σ_μ^2 = overall variance of the area density irregularity

σ_a^2 = variance due to the random component

σ_p^2 = variance due to the periodic component

ρ_a = autocorrelation function of the random component

ρ_p = autocorrelation function of the periodic component

The figure [28] shows that the standardized form of the variance composition can be written as follows:

$$\beta(A) = \eta \cdot \beta_p(A) + (1-\eta) \cdot \beta_a(A) \tag{43}$$

The extension of the above results to the more general case of the superposition of n sinusoidal type irregularities can be written as follows:

$$M(x) = \mu_a(x) + \sum_1^n a_i \cos(\omega_i x + \phi_i) \tag{44}$$

where $\mu_a(x)$ is the random component and the following term $(\sum_1^n a_i \cos(\omega_i x + \phi_i)$ is the element due to Fourier series developments of the periodic components. Hence

$$\beta(A) = \sum_1^n \left[\eta_i \cdot \beta_{p_i}(A) \right] + \left(1 - \sum_1^n \eta_i \right) \cdot \beta_a(A) \tag{45}$$

η_i being the weighting factor for the periodic component of rank i.

Figures 15 and 16 show some simulation examples of compositions of one or two sinusoidal irregularities with a random irregularity (isoprobable distribution). The interpretation of the curves $\beta(A)$ respectively $\gamma(A)$ becomes much more difficult. Of course the presence of "arches" or "sinuosities" indicates the presence of periodic irregularity.
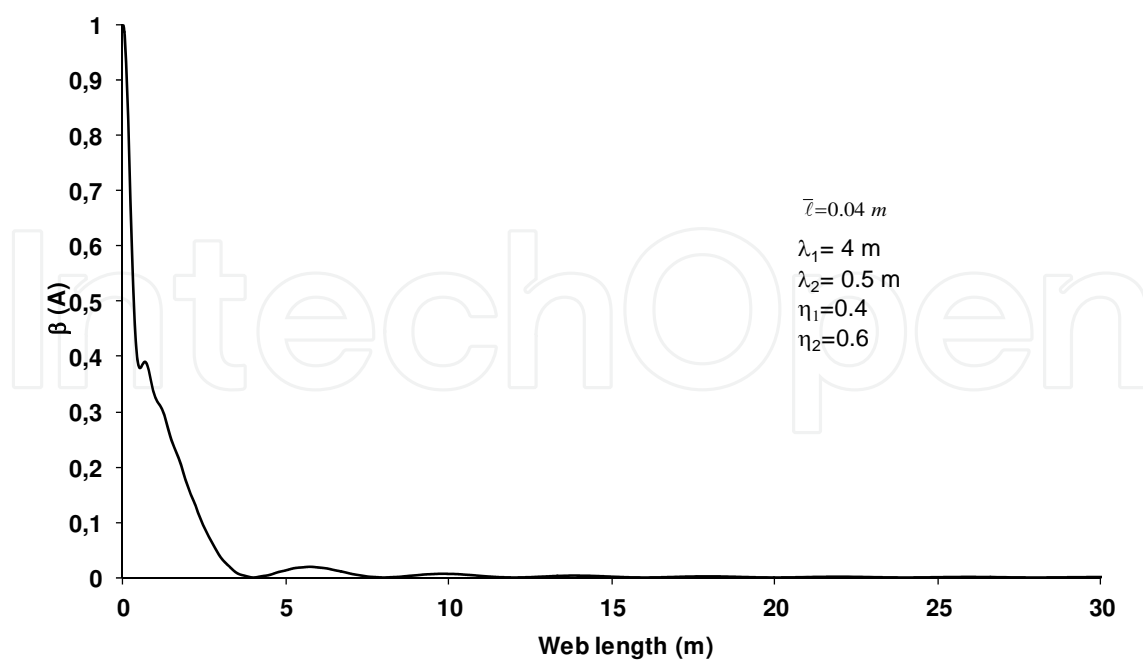
Figure 15. Normalized between-area-density variance curve – compound irregularity
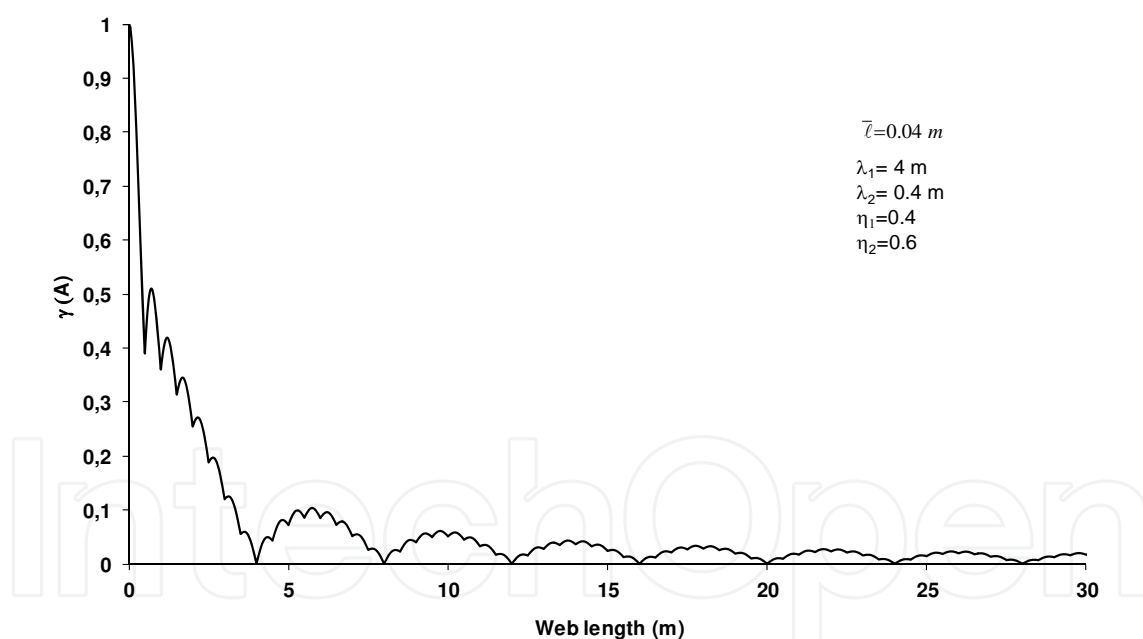

Figure 16. Normalized between-area-density variance coefficient curve – compound irregularity.

6. Conclusion

Nonwoven industries are fiber-based industries. Based on their physical and mechanical properties, the nonwoven applications are increasing inducing a strong growth of the non-

woven production. The physical and mechanical properties of these products strongly depend on the evenness of laps or webs. Thus, the nonwoven manufacturers absolutely need tools to evaluate these properties. Hence, an accurate knowledge of the web and lap formation as well as the associated theoretical approach is absolutely necessary. In this paper we propose a theoretical approach simulating the real faults of the fiber-web forming-step during the industrial process. Thanks to this theory, we were able to calculate from measurements both the random and periodic components of the real defects for all textile types as fibrous webs and nonwovens. The periodic component depends on the production machine and the random component depends mainly on the characteristics of the fibers. In this study, we are not interested in uniformity of the visual appearance (2-D uniformity) of the fiber web but we assess the 3-D uniformity from the area density. This uniformity is determined from small surface-elements and not from image analysis [16,24]. We did not analyze the correlation between the irregularity of the yarns and the woven fabric [20] but measured directly surface and mass irregularities thereof. This involves the use of specific sensors (such as capacitive, ultrasonic, and radioactive sensors). To highlight these irregularities (random or periodic), the fiber web is divided into several elements that have the same surface. Then the between-area-density variance function is defined with the help of the autocorrelation function. The common distribution functions of the fiber flocks are used to carry out the random component of the equation. Finally, according to the law of additive covariances composition, periodic defects have been added to the random component in order to determine the theoretical equation. This information is fundamental to the production manager in order to detect the earliest possible manufacturing breakdown and to optimize the machine settings and textile production quality.

Author details

Jean-Yves Drean and Omar Harzallah[*]

*Address all correspondence to: o.harzallah@uha.fr

Université de Haute Alsace – Laboratoire de Physique et Mécanique Textiles, Mulhouse, France

References

[1] S. J. Russell, *Handbook of nonwovens*, The Textile Institute, Woodhead Publishing Limited, Cambridge, England, 2007.

[2] G. Tanchis, *Reference book of textile technologies: the nonwovens*, Fondazione ACIMIT, Italy, 2008.

[3] R. A. Chapman, *Applications of nonwovens in technical textiles*, Woodhead Publishing Limited, Cambridge, England, 2010.

[4] W. Albrecht, H. Fuchs and W. Kittelmann, *Nonwoven fabrics,* WILEY-VCH Verlag GmbH & Co. KGaA, Weinheim, 2003.

[5] R. M. Koerner, *Designing with geosynthetics*, Second Edition, Prentice-Hall, Engle-wood Cliffs, 1990.

[6] J. L. Spencer-Smith and H. A. C. Todd, A time series met with in textile research. Supplement to the *Journal of the Royal Statistical Society*, 7(2), 131-145, 1941.

[7] J. G. Martindale, A new method of measuring the irregularity of yarns with some ob-servations on the origin of irregularities in worsted slivers and yarns. *Journal of the Textile Institute*, 36, T35-47, March 1945.

[8] M. W. H. Townsend and D. R. Cox, The analysis of yarn irregularity. *Journal of the Textile Institute,* 42, P107-113, 1951.

[9] M. W. H. Townsend and D. R. Cox, The use of correlograms for measuring yarn ir-regularities. *Journal of the Textile Institute*, 42, P145-151, 1951.

[10] H. Breny, The calculation of the variance-length curve from the length distribution of fibers. *The Journal of the Textile Institute*, Part I, 44, P1-P9, January 1953.

[11] H. Breny, The calculation of the variance-length curve from the length distribution of fibers. *Journal of the Textile Institute*, Part II, 44, P10-P14, January 1953.

[12] P. Grosberg and R. C. Palmer, On the determination of the B-L curve by cutting and weighing. *Journal of the Textile Institute*, 4(45), April 1954.

[13] P. Grosberg, The medium and long-term variations of yarn. *Journal of the Textile Insti-tute*, 46, T301-T309, May 1955.

[14] A. Kirschner, R. Petiteau and R. A. Schutz, Contribution à l'Analyse Spectrale des Structures Textiles Linéaires. *Bulletin Scientifique ITF*, 19(5), Août 1976.

[15] W. Wegener, The irregularity of woven and knitted fabrics. *Journal of the Textile Insti-tute*, 77(2), 69-75, March-April 1986.

[16] Y. Wu, B. Pourdeyhimi and M. S. Spivak, Textural evaluation of carpets using image analysis. *Textile Research Journal*, 61, 407-419, 1991.

[17] E. J. Wood, Applying Fourier and associated transforms to pattern characterization in textiles. *Textile Research Journal*, 60, 212-220, 1990.

[18] D. Han, *Development of fabric image models and invariance property of variance-area curve within fabric*. Master's thesis, NCSU, College of Textiles, Raleigh, 2002.

[19] M. W. Suh, M. Günay and W. J. Jasper, Prediction of surface uniformity in woven fabrics through 2-D anisotropy measures, Part I: Definitions and theoretical Model. *Journal of the Textile Institute*, 98(2), 109-116, 2007.

[20] M. Günay, M. W. Suh and W. J. Jasper, Prediction of surface uniformity in woven fabrics through 2-D anisotropy measures, Part II: Simulation and verification of the prediction model. *Journal of the Textile Institute,* 98(2), 117-126, 2007.

[21] P. Andrianarisoa, M. Averous, J. Y. Drean and R. A. Schutz, Evaluation de la Distribution de la Masse Surfacique des Fibres dans les Textiles Surfaciques. *Bulletin Scientifique ITF*, 51(13), 3-19, 1984.

[22] A. Cherkassky, A two-dimensional mathematical model of the carding process. *Textile Research Journal*, 64(3), 169-175, 1994.

[23] R. K. Aggarwal, W. R. Kennon and I. Porat, Scanned-laser technique for monitoring fibrous webs and nonwoven fabrics. *Journal of the Textile Institute,* 83(3), 386-398, 1992.

[24] A. Cherkassky, Analysis and simulation of nonwoven irregularity and nonhomogeneity. *Textile Research Journal*, 68(4), 242-253, 1998.

[25] A. Cherkassky, Analysis of the smoothing effect of the card cylinder using simulation. *Textile Research Journal*, 65(12), 723-730, 1995.

[26] Papoulis, *Probability, random variables and stochastic processes*, McGraw-Hill, New-York, 1968.

[27] A. Kirschner, Contribution à l'Etude des Variables et Processus Aléatoires Associés aux Structures Textiles Linéaires. D.Sc., Université de Haute Alsace, 87MULH47, 1987.

[28] J. Y. Drean, et M. Renner, Contribution à l'Etude Théorique et Expérimentale du Processus d'Obtention des Textiles Linéaires. D.Sc., Université de Haute Alsace, 86MULH19, 1986.

[29] J. Y. Drean, O. Harzzallah and M. Renner, Textile surfaces analysis and modelling based on statistical methods: Variance analysis and autocorrelation functions. *Textile Research Journal*, 80(17), 1833-1845, 2010